Journal of Statistical Physics, Vol. 128, Nos. 1/2, July 2007 (© 2007)
DOI: 10.1007/s10955-006-9249-x

Switching Statistics of a Flagellar Motor: First-Passage Time and Dynamic Binding

Qi Wen,[1] Guanglai Li,[1] Jay X. Tang[1] and Greg Huber[2,3]

Received February 6, 2006; accepted October 26, 2006
Published Online January 5, 2007

Bacterial chemotaxis relies on the clockwise-to-counterclockwise switching (and the reverse CCW-to-CW switching) of the flagellar motor's rotational direction. Yet, despite its central role, the switch mechanism remains poorly understood. Here we study the switch statistics of the flagellar motor using computer simulations that combine first-passage time ideas and the property of dynamic binding of CheY-P to FliM. The simulated clockwise bias and switching frequency as a function of CheY-P concentration agree with the experimental results for *E. coli*. Moreover, the simulation results show a robust peak, which is present in some experimental reports, in the distribution of the time intervals of both clockwise and counterclockwise rotation.

KEY WORDS: molecular motors, flagellar motor, first-passage time, chemotaxis, dynamic binding, molecular switch, switching statistics

1. INTRODUCTION

The flagellar motor of bacteria is perhaps the most elaborate stoichiometric molecular machine engineered by evolution. The motor harnesses the chemical energy associated with a proton (or sodium) gradient for its rotation (typically hundreds of Hz), while, at longer time scales, stochastically switching between clockwise (CW) and counterclockwise (CCW) rotations. The rotation drives the bacterium's directional motility, but the switching also plays a crucial role, particularly in chemotaxis.[1,2] Switching is controlled by the C-ring, the switch complex of the motor, which is composed of the proteins FliM, FliN, and FliG. There are about 34 FliM proteins in the C-ring.[3,4] The phosphorylated form of CheY, CheY-P,

[1] Department of Physics, Brown University, Providence, RI 02912.
[2] Center for Cell Analysis & Modeling, Department of Cell Biology, University of Connecticut Health Center, Farmington, CT 06030; e-mail: huber@uchc.edu.
[3] Department of Mathematics, University of Connecticut, Storrs, CT 06269.

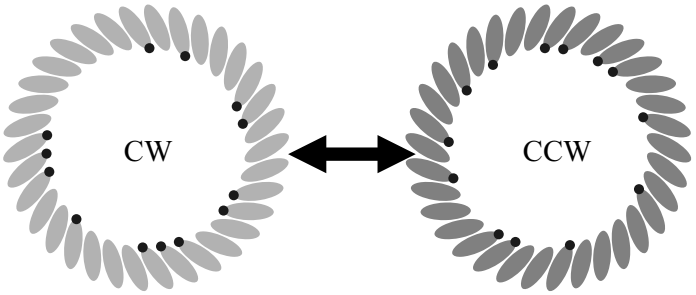

Fig. 1. Schematic drawing of the 34 FliM proteins in the C-ring when the motor rotates CW (*light gray*) or CCW (*dark gray*). CheY-P proteins (black circles) are bound to some of the FliM proteins.

binds to the protein FliM, and thereby regulates the switching of the motor.[5,6] The distribution of the intervals of CW and CCW rotation provides insight into the switching mechanism. For *E. coli*, that distribution has been observed to follow an exponential-decay form,[7] and a two-state model[8] is often invoked to understand this distribution. Such a model assumes a free energy for each of the CW and CCW rotational states with an energy barrier between them, and it follows from this model that the interval distributions of CW and CCW rotation decay exponentially.[7] Mogilner *et al*.[9] modified the two-state model by using two free-energy wells, arrayed along a reaction coordinate, to represent the two stable rotation states of the flagellar motor. The motor state diffuses along the coordinate connecting the energy wells, and switching occurs when the motor reaches the top of the intervening energy barrier. The interval is then taken as the first-passage time for a motor starting at the bottom of a well to reach the barrier height. The probability distribution of interval size obtained from this model has a peak at very short intervals, with the probability density at interval size zero being zero. After the peak, it decays nearly exponentially. However, this model didn't consider the stochastic process of CheY-P binding to FliM. To take into account the dynamic binding of CheY-P, in this paper, we use a Langevin-equation approach and first-passage time theory[10] to simulate the switching events in *E. coli*, basing our model on the molecular structure of the switch complex.

2. SIMULATION

2.1. Model

Each FliM has two stable conformational states that correspond to the clockwise and counterclockwise rotation of the motor, respectively. CheY-P binds to individual FliM units, and promotes their CW state. A FliM without CheY-P bound is stable in its CCW state. To capture this effect, the free energy of a single FliM

unit is assumed to take the following form:

$$g(x) = 4\,\delta g_b \left(\frac{x^4}{4} - \frac{x^2}{2}\right) \pm \frac{\delta g}{2} x \tag{1}$$

where x is a generalized coordinate representing the conformational change of a FliM, δg is the free-energy difference between the CW state and CCW state, and δg_b is a simulation coefficient related to the height of the energy barrier. For a FliM without a CheY-P bound, the negative sign is applied in Eq. (1); otherwise the positive sign is applied.

We shall assume that the FliM units are so strongly correlated that their motions in their reaction coordinates can be reduced to motion in one variable, *i.e.* $x = x_i$ ($i = 1, 2, \ldots, 34$), where the coordinate x now represents the entire switch complex. This is a strong assumption which adopts the philosophy of the model of Mogilner *et al.*[11] Another assumption of our model is that the correlations between individual FliM units are insensitive to state of CheY-P binding and the state of the FliM unit. Therefore, the free energy of the switching complex due to the correlations between FliM units does not vary with CheY-P binding and the switching of the motor. The correlation energy, however large, would only add a constant and thus not affect the switch energetics. Neglecting this constant, and summing up the free energy of the individual FliM units ($G = \sum_{i=1}^{34} g(x_i)$), the total free energy of the switch complex can then be written as:

$$G(x) = 4\,\Delta G_b \left(\frac{x^4}{4} - \frac{x^2}{2}\right) - \frac{\Delta G}{2} x \tag{2}$$

where $\Delta G = (34 - 2N)\,\delta g$, and $\Delta G_b = 34\,\delta g_b$. Note that $G(x)$ contains a functional dependence on N, the number of FliM units occupied by CheY-P. In the absence of CheY-P ($N = 0$), the free energy of the CW state is approximately $14\,k_B T$ higher than that of the CCW state.[11] δg is then estimated to be $\frac{14}{34}\,k_B T = 0.42\,k_B T$. When 17 of the 34 FliM units are occupied by CheY-P, $\Delta G = 0$, the barrier height is ΔG_b, and the maximum of the barrier is located at $x = 0$ (see Fig. 2).

The binding of CheY-P to FliM is a dynamic process. A bound CheY-P dissociates from a FliM at a rate k_{off}, the value of which has been measured to be $30\,\text{s}^{-1}$ in *E. coli*,[12] and a free CheY-P binds to an unoccupied FliM at a rate k_{on}. The two rates are related in such a way that $k_{\text{off}} N = k_{\text{on}}(34 - N)$, where N is the average number of FliM occupied by CheY-P under a certain CheY-P concentration.

To simulate the dynamic binding process, initially N of the FliM units are randomly selected to be occupied with CheY-P. After each time step, Δt, a bound CheY-P dissociates from the FliM with a probability of $p_{\text{off}} = 1 - e^{-k_{\text{off}}\Delta t}$, while the probability for an unoccupied FliM to trap a free CheY-P is $p_{\text{on}} = 1 - e^{-k_{\text{on}}\Delta t}$. To determine if a bound CheY-P dissociates, a random number $a \in [0, 1]$ is

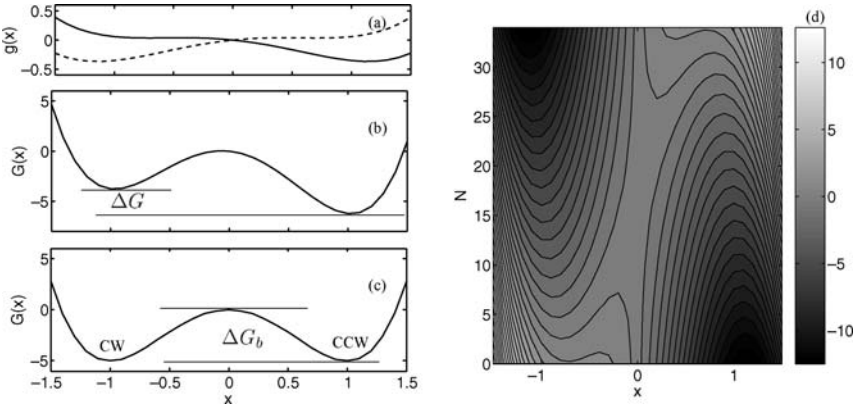

Fig. 2. Free energy of (a) single FliM unit with a CheY-P bound (*dashed line*) and without CheY-P (*solid line*) as a function of x; (b) switch complex with $\Delta G_b = 5.0\,k_{\rm B}T$, $N = 14$; (c) switch complex with $\Delta G_b = 5.0\,k_{\rm B}T$, $N = 17$; (d) contour plot of $G(x)$ as a function of x, and N.

generated and compared with $p_{\rm off}$. If $p_{\rm off} > a$, the CheY-P dissociates, otherwise it remains bound. The same algorithm is used to determine if an unoccupied FliM traps a free CheY-P. Figure 3a displays the results of the fluctuations in N in a 2-s time window. The fluctuations of N create variations in ΔG, and thus generate a fluctuating potential $G(x)$. This fluctuating $G(x)$ makes a simulation based on the master equation inordinately complicated.[9,13] Therefore, we take a new approach to the problem by combining first-passage time theory and numerical solution of the Langevin equation.

2.2. Langevin Equation

Driven by thermal noise, the switch complex diffuses under the influence of the fluctuating potential $G(x)$. The motion of the switch complex can be represented by an overdamped Langevin equation:

$$\frac{dx}{dt} = -\frac{1}{\zeta}\frac{dG(x)}{dx} + \frac{1}{\zeta}\eta(t) \tag{3}$$

where $\eta(t)$ is a time-dependent random "Brownian force," and ζ is the generalized frictional coefficient.

Integrating both sides of Eq. (3) over a time interval $(t, t + \Delta t)$, we get:

$$x(t + \Delta t) = x(t) - \frac{1}{\zeta}\int_t^{t+\Delta t}\frac{dG(x)}{dx}dt' + \frac{1}{\zeta}\int_t^{t+\Delta t}\eta(t')dt'$$

Within a short time interval, $\Delta t \ll 1/k_{\rm off}$, the potential does not fluctuate, and the first integration can be approximated by $\Delta t\,\frac{dG(x)}{dx}|_{x=x(t)}$, using Euler's method. The

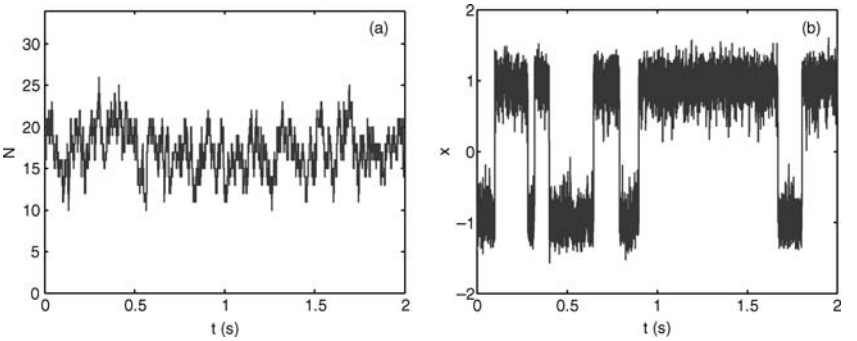

Fig. 3. (a) Fluctuation of N at an off rate of $k_{\text{off}} = 30\,\text{s}^{-1}$; the number of CheY-P at the beginning of the simulation is 17. (b) Sample trace of the switch complex diffusing under the influence of $G(x)$, with $N = 17$, $D = 70$, and $k_{\text{off}} = 30\,\text{s}^{-1}$.

third term is the effect of Brownian noise in this time interval. It can be simulated by a random term $\sqrt{2D\Delta t}\,\xi$, where ξ is a normally-distributed random variable with mean 0 and variance 1. Equation (3) is then approximated as follows:

$$x(t + \Delta t) = x(t) - \frac{d\bar{G}(x)}{dx} D\Delta t + \sqrt{2D\Delta t}\,\xi \tag{4}$$

where $\bar{G}(x) \equiv G(x)/k_{\text{B}}T$. Numerical implementation of Eq. (4) is straightforward. Figure 3b shows a sample time series of the switch coordinate under the fluctuating potential $G(x)$. To generate this trace, the average number of FliM occupied by CheY-P is $N = 17$, diffusion constant is $D = 70$, and $\Delta G_b = 5\,k_{\text{B}}T$.[11]

From the recorded trace, we can get the average time intervals for both the CW and CCW states of the switch complex. In the simulation, an absorbing boundary condition is applied at the top of the barrier between the CW and CCW states. The switch complex starts from the equilibrium position of one state, and when it reaches the summit of the barrier, it is immediately reset to the equilibrium position of the other state. Using this technique, we record the first-passage times for each state to pass over the energy barrier, and these times are compiled to plot the interval distribution function.

Although the numerical procedure presented here does not strictly preserve detailed balance,[9,13] by taking into account the dynamic binding of CheY-P to FliM, it has the advantage of simulating the fluctuating potential $G(x)$. Moreover, the finite current that signals the breakdown of detailed balance, and which results from numerical error in the Euler step, can be made vanishingly small for small time steps Δt. The current is defined as $j(x) = -D(\bar{G}'(x)\rho(x) - \rho'(x))$, where $\rho(x)$ is the probability density for a FliM to stay at x, and $\bar{G}'(x)$ and $\rho'(x)$ are the derivatives of $\bar{G}(x)$ and $\rho(x)$, respectively.[13] In Fig. 4, we show how this current decreases with the size of the time step, choosing parameters identical to those

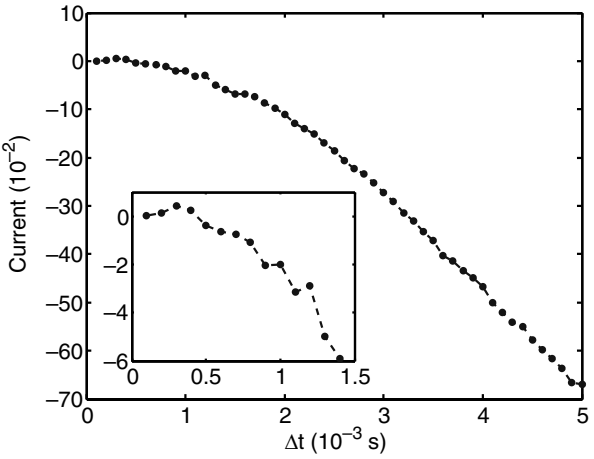

Fig. 4. Current decreases as the simulation time step decreases. The inset shows the current at short time steps: $0.0001\,\text{s} \leq \Delta t \leq 0.0015\,\text{s}$, detailing its decrease to negligible values as $\Delta t \to 0.0001\,\text{s}$.

of Elston and Doering.[13] To verify our algorithm, we have compared the results generated by turning off the dynamic binding process to the interval distribution generated by the master equation using the same parameters. Both methods give identical mean first-passage times and peak positions close to zero time interval. In the next section, we discuss the importance of the dynamic binding, which has not been treated by previous master-equation methods.

3. RESULTS AND DISCUSSION

3.1. Dynamic Binding

The dynamic binding of CheY-P causes fluctuations in the potential $G(x)$. From Eq. (2), variations in the number of CheY-Ps bound to the C-ring not only changes the free-energy difference between the CW and CCW states, but also shifts the position of the maximum point on the barrier. Both of these changes affect the amount of time required for the switch complex to move across the top of the barrier, and thus give rise to a peak in the interval distributions which is qualitatively different from that predicted in previous studies.[9]

Figure 5 shows a comparison between the results of simulations with and without dynamic binding of CheY-P. A peak is observed in both situations. Peaks have been intermittently reported in several experiments, but at times viewed as experimental artifacts, perhaps because previous theory has either predicted no peak, or a peak very close to zero interval and beyond the resolution of

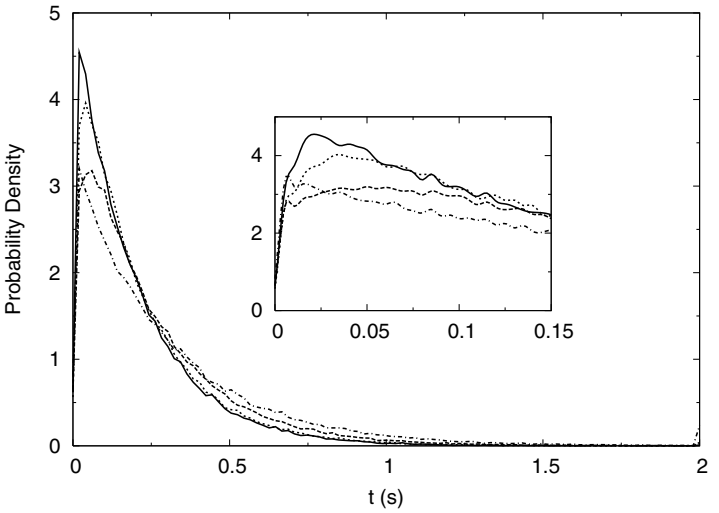

Fig. 5. Distribution of first-passage times. Lines are for $k_{\text{off}} = 0$ (*dash dotted*), 10 (*dotted*), 30 (*dashed*), and 60 (*solid*) s^{-1}, respectively. The corresponding peaks are located at approximately $t = 0.01,\ 0.05,\ 0.04,\ 0.03\,\text{s}$. The other parameters are set to $N = 17$, $D = 70$, $\Delta G_b = 5\,k_{\text{B}}T$, and $dt = 0.0001\,\text{s}$. Inset: a magnified view of the range between 0 and 0.15 s.

experimental technique. However, a robust peak has been observed in recent experiments.[14–17] With dynamic binding, the peak in interval distribution is shifted towards larger time intervals, leading to the prediction of an observable peak. It is interesting to note that this shift in peak position does not move to arbitrarily-large time intervals at greater values of k_{off}. Instead, the peak position increases from 0.01 to 0.05 s when k_{off} increases from 0 to 10 s^{-1}, and then moves back towards zero as k_{off} increases further.

3.2. Peak Position

Figure 6 shows the dependence of peak positions upon the value of N, the number of occupied FliM units. The peak time intervals for the CW distributions increase with increasing N, while the peak time intervals for the CCW case decrease as N increases.

First-passage concepts can account for this N dependence. The peak position of the first-passage time distribution for freely-diffusing particles depends only on the diffusion constant and the threshold for first-passage.[10] A larger threshold moves the peak towards larger time intervals. In our simulation, the CW interval is the first-passage time for a switch complex to move from its CW equilibrium position to the point of maximum energy barrier. At larger N, as shown in Fig. 2,

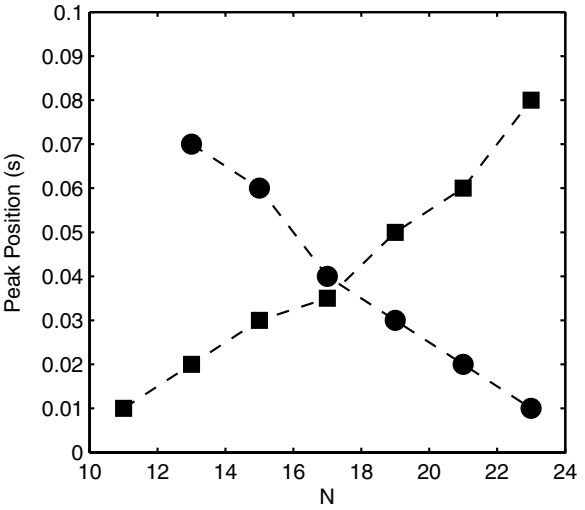

Fig. 6. Peak position as a function of N. As N increases, the time intervals for the peak positions of CW-interval distributions (*squares*) increase, and the time intervals for peak positions of CCW distributions (*circles*) decrease. The other simulation parameters are set to: $k_{\text{off}} = 30\,\text{s}^{-1}$, $D = 70$, $\Delta G_b = 5\,k_{\text{B}}T$, and $dt = 0.0001\,\text{s}$.

the distance between the CW equilibrium position and the position of the barrier is greater. Hence, an increase in N gives rise to a CW-interval distribution with a peak at a larger time interval. Likewise, increasing N results in peak positions decreasing for CCW intervals.

3.3. CW Bias and Switching Frequency

Figure 7a shows bias as a function of average FliM occupancy N. The bias is not sensitive to the diffusion constant or the rate of CheY-P falling off from FliM. CW bias is defined as the ratio of average CW interval to the sum of average CW and CCW intervals:

$$\text{bias} = \frac{\langle t_{cw} \rangle}{\langle t_{cw} \rangle + \langle t_{ccw} \rangle}$$

where $\langle t_{cw} \rangle$ and $\langle t_{ccw} \rangle$ are the average interval size for CW and CCW states, respectively. From the point of view of statistics, the bias is the probability for the switch complex to stay in the CW state. Assuming the free energy level of CW and CCW states are G_{cw} and G_{ccw}, respectively. The CW bias could be written as

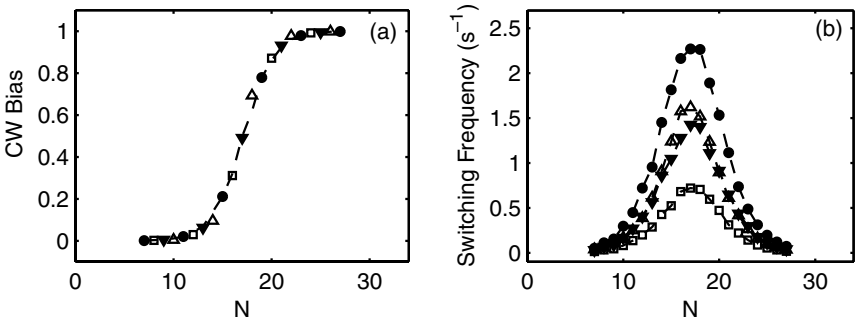

Fig. 7. CW bias and switching frequency as a function of N. $D = 70, k_{\text{off}} = 30$ (*solid circles*); $D = 70, k_{\text{off}} = 0$ (*open up triangles*); $D = 40, k_{\text{off}} = 30$ (*open squares*); $D = 20, k_{\text{off}} = 30$ (*solid down triangles*).

follows:

$$\text{bias} = \frac{e^{-\frac{G_{cw}}{k_{\text{B}}T}}}{e^{-\frac{G_{cw}}{k_{\text{B}}T}} + e^{-\frac{G_{ccw}}{k_{\text{B}}T}}} = \frac{1}{1 + e^{\frac{\Delta G}{k_{\text{B}}T}}}$$

The bias gives information only on the difference in free energy ΔG between the CW and CCW states. From Eq. (2), ΔG is sensitive to the FliM occupancy N, and is not sensitive to the diffusion constant. Under a certain CheY-P concentration, the FliM occupancy fluctuates at a different rate under different k_{off} values. However, the average number N of CheY-P on a switch complex does not change with k_{off}, which means the average value of ΔG is not sensitive to k_{off}. Therefore, in Fig. 7a, results of simulation with dynamic binding are essentially the same as those of simulations without dynamic binding.

Another important descriptive parameter is the switching frequency. Switching frequency is inversely related to the average time intervals. Experimentally, this means the number of observed switches per unit time. In the simulation, we calculated the mean first-passage time for the two states. When the switch complex reaches the summit of the barrier, the probability for it to switch to the other state is only 50%. Hence, the real interval is twice the simulated mean first-passage time,[11] and the switching freqency is then calculated as:

$$f = \frac{1}{\langle t_{cw} \rangle + \langle t_{ccw} \rangle}$$

In Fig. 7b, the switching frequency is quite sensitive to the diffusion constant and k_{off}. A larger diffusion constant or a greater k_{off} value leads to a higher switching frequency. This is because the absolute value of the first-passage time is determined

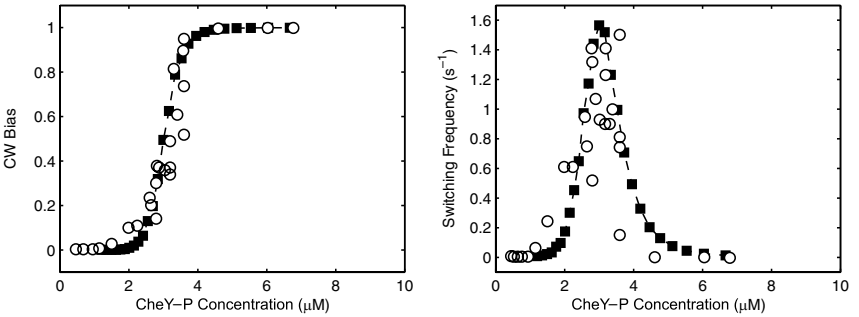

Fig. 8. Comparison of experimental data [18] (*open circles*) with simulation results (*solid squares*). Parameters used in the simulation are: $D = 70$, $k_{\text{off}} = 30\,\text{s}^{-1}$, and $\Delta G_b = 5\,k_{\text{B}}T$.

by the diffusion constant and details of the fluctuations of $G(x)$. The faster $G(x)$ fluctuates, the higher the chance for a switch to take place within a shorter period time.

To explore the connection between CW bias and CheY-P concentration, we use the relation between N and the CheY-P concentration extracted from the experimental results:[12]

$$[\text{CheY-P}] = K_D \left(\frac{N}{34 - N} \right)^{1/2.2}$$

where $K_D = 3.0\,\mu$M, and the CheY-P concentration is also in the unit of μM. The value of K_D is close to the experimental value $3.2\,\mu$M [12]. In Fig. 8, we show that our simulation results on both the CW bias and switching frequency qualitatively agree with the experiments.[18]

4. CONCLUSION

We have studied the switching events in a model of the bacterial flagellar motor using computer simulations based on first-passage time theory and on a molecular picture of the switch complex, taking into account the dynamic binding of CheY-P to FliM. The results are in good agreement with experiments on *E. coli*. A peak is observed in the interval distribution, which can be viewed as a robust result of the first-passage time theory. Without the effects of dynamic binding, the peak is shifted to such short time intervals as to be impossible to resolve practically in current experiments. Recent experiments, by contrast, show a clear peak in the interval distribution for *E. coli* [16] and *Caulobacter crescentus*.[18] This points to an important role for dynamic binding in the motor switching mechanism.

ACKNOWLEDGMENTS

We appreciate discussions with R. Mukhopadhyay, H. C. Berg, and T. R. Powers. This work was supported by NSF DMR 0405156 (JXT), by a Galkin graduate fellowship (QW), and by the Richard Berlin Center for Cell Analysis & Modeling (GH).

REFERENCES

1. H. C. Berg, *Annu. Rev. Biochem.* **72**:19 (2003).
2. H. C. Berg, *E. coli in Motion* (Springer, New York, 2004).
3. D. R. Thomas, D. G. Morgan and D. J. DeRosier, *Proc. Natl. Acad. Sci.* **96**:10134 (1999).
4. H. S. Young, H. Dang, Y. Lai, D. J. DeRosier and S. Khan, *Biophys. J.* **84**:571 (2003).
5. B. E. Scharf, K. A. Fahrner, L. Turner and H. C. Berg, *Proc. Natl. Acad. Sci.* **95**:201 (1998).
6. M. Montrone, M. Eisenbach, D. Oesterhelt and W. Marwan, *J. Bacteriol.* **180**:3375 (1998).
7. S. M. Block, J. E. Segall and H. C. Berg, *J. Bacteriol.* **154**:312 (1983).
8. S. Khan and R. M. Macnab, *J. Mol. Biol.* **138**:563 (1980).
9. A. Mogilner, T. C. Elston, H. Wang and G. Oster, *Computational Cell Biology*, In C. P. Fall, E. S. Marland, J. M. Wagner, and J. J. Tyson (eds.), p. 321 (Springer-Verlag, New York, 2002).
10. S. Redner, *A Guide to First-Passage Processes* Cambridge University Press, Cambridge (2001).
11. A. Mogilner, T. C. Elston, H. Wang and G. Oster, *Computational Cell Biology*, In C. P. Fall, E. S. Marland, J. M. Wagner, and J. J. Tyson (eds.), p. 354 (Springer-Verlag, New York, 2002).
12. V. Sourjik and H. C. Berg, *Proc. Natl. Acad. Sci.* **99**:12669 (2002).
13. T. C. Elston and C. R. Doering, *J. Stat. Phys.* **83**:359 (1996).
14. E. Korobkova, T. Emonet, J. M. Vilar, T. S. Shimizu and P. Cluzel, *Nature* **428**:574 (2003).
15. Y. Magariyama, S. Masuda, Y. Takano, T. Ohtani and S. Kudo, *FEMS Microbiol. Lett.* **205**:343 (2001).
16. E. A. Korobkova, T. Emonet, H. Park and P. Cluzel, *Phys. Rev. Lett.* **96**:058105 (2006).
17. G. Li, Q. Wen, J. X. Tang and G. Huber (unpublished).
18. P. Cluzel, M. Surette and S. Leibler, *Science* **287**:1652 (2000).